

Article

Green-Synthesized Zinc Oxide Nanoparticles Mitigate Salt Stress in *Sorghum bicolor*

Tessia Rakgotho ^{1,2}, Nzumbululo Ndou ^{1,2}, Takalani Mulaudzi ^{1,*}, Emmanuel Iwuoha ²,
Noluthando Mayedwa ² and Rachel Fanelwa Ajayi ²

¹ Life Sciences Building, Department of Biotechnology, University of the Western Cape, Private Bag X17, Bellville 7535, South Africa; 3985506@myuwc.ac.za (T.R.); 3992677@myuwc.ac.za (N.N.)

² SensorLab, Department of Chemical Sciences, University of the Western Cape, Private Bag X17, Bellville 7535, South Africa; eiwuoha@uwc.ac.za (E.I.); 2548096@myuwc.ac.za (N.M.); fngece@uwc.ac.za (R.F.A.)

* Correspondence: tmulaudzi@uwc.ac.za; Tel.: +27-219-592-557

Abstract: Salinity is an abiotic stress that is responsible for more than 50% of crop losses worldwide. Current strategies to overcome salinity in agriculture are limited to the use of genetically modified crops and chemicals including fertilizers, pesticides and herbicides; however these are costly and can be hazardous to human health and the environment. Green synthesis of nanoparticles (NPs) is an eco-friendly and cost-effective method, and they might serve as novel biostimulants. This study investigated for the first time the efficiency of ZnO NPs, synthesized from *Agathosma betulina* to mitigate salt stress in *Sorghum bicolor*. Hexagonal wurtzite ZnO NPs of about 27.5 nm, were obtained. Sorghum seeds were primed with ZnO NPs (5 and 10 mg/L), prior to planting on potting soil and treatment with high salt (400 mM NaCl). Salt significantly impaired growth by decreasing shoot lengths and fresh weights, causing severe deformation on the anatomical (epidermis and vascular bundle tissue) structure. Element distribution was also affected by salt which increased the Na⁺/K⁺ ratio (2.9). Salt also increased oxidative stress markers (reactive oxygen species, malondialdehyde), enzyme activities (SOD, CAT and APX), proline, and soluble sugars. Priming with ZnO NPs stimulated the growth of salt-stressed sorghum plants, which was exhibited by improved shoot lengths, fresh weights, and a well-arranged anatomical structure, as well as a low Na⁺/K⁺ ratio (1.53 and 0.58) indicating an improved element distribution. FTIR spectra confirmed a reduction in the degradation of biomolecules correlated with reduced oxidative stress. This study strongly suggests the use of green-synthesized ZnO NPs from *A. betulina* as potential biostimulants to improve plant growth under abiotic stress.

Keywords: abiotic stress; green synthesis; priming; osmolytes; oxidative stress; salt; sorghum; buchu extract; ZnO NPs; antioxidant



Citation: Rakgotho, T.; Ndou, N.; Mulaudzi, T.; Iwuoha, E.; Mayedwa, N.; Ajayi, R.F. Green-Synthesized Zinc Oxide Nanoparticles Mitigate Salt Stress in *Sorghum bicolor*.

Agriculture **2022**, *12*, 597. <https://doi.org/10.3390/agriculture12050597>

Academic Editors: Daniele Del Buono, Primo Proietti and Luca Regni

Received: 14 March 2022

Accepted: 21 April 2022

Published: 24 April 2022

Publisher's Note: MDPI stays neutral with regard to jurisdictional claims in published maps and institutional affiliations.



Copyright: © 2022 by the authors. Licensee MDPI, Basel, Switzerland. This article is an open access article distributed under the terms and conditions of the Creative Commons Attribution (CC BY) license (<https://creativecommons.org/licenses/by/4.0/>).

1. Introduction

Nanotechnology is an emerging technology that has recently led to the synthesis of nano compounds (nanomaterials and nanoparticles) with special properties and the potential to be used as plant growth regulators and biostimulants in agriculture [1,2]. A few studies have demonstrated the effective use of different nanoparticles in the improvement of crop production under abiotic stresses [3–8]. Hence nanotechnology can be used in agriculture to meet targets in food production to feed the growing population [1].

Green synthesis of nanoparticles must be considered as the method of choice for plant application, due to its several advantages over conventional methods, since it is cost effective, eco-friendly, and can be easily scaled-up for increased production [9]. Additionally, there is no usage of high temperatures, energy, pressure, and toxic chemicals in green synthesis [10]. Plant extracts are the most common biological substrates used in the synthesis of nanoparticles since they are easily accessible and less toxic than microbes. These extracts

contain secondary metabolites such as polysaccharides, polyphenolic compounds, amino acids, vitamins, and alkaloids among other compounds that act as reducing, stabilizing, and capping agents [11,12].

Metal oxide nanoparticles, specifically Zinc oxide nanoparticles (ZnO NPs) have recently gained a lot of attention in nanoscience due to their unique physicochemical properties and their various applications in biology, chemistry, medicine, and physics [11,13–15] and in recent years they have crossed over to agriculture [16,17]. Zinc oxide is nonorganic, cheap, and it has been regarded as a safe and non-toxic metal by the Food and Drug Administration (FDA). Several studies have revealed that a lower concentration of ZnO NPs can increase the growth and development of plants [18,19].

Salinity is among the major abiotic stresses that affect plant growth and development by altering several physiological and metabolic processes of plants [20–23]. It has affected approximately 6% of the total land surface globally and 20% of agricultural land, making salt stress the most serious environmental factor limiting the productivity of cultivated crops [24]. Salinity causes osmotic and ionic stress, which enhances the over-production of reactive oxygen species (ROS) causing lipid membrane damage, damage to biomolecules, and hence, cell death [23,25]. Plants overcome these effects by regulating several defense mechanisms including osmotic adjustments, induction of the antioxidant machinery, modulation of hormones, and some morphological and anatomical adaptations [23,26]

Sorghum bicolor (L.) Moench is an important grain crop ranked fifth in the world and second in Africa [24]. In African and Asian countries, sorghum is mainly used as a source of food for humans, whereas in other countries such as Australia, Brazil, and the United States of America, it is mostly used as a source of animal feed and energy production. It is an adaptable and a moderately drought and salt-tolerant cereal crop [27,28]; however, continuous exposure to abiotic stress can affect its growth and hence its productivity. Cultivating sorghum is very important because this will ensure its continuous use as a food source to combat food insecurity and in the production of bioenergy to solve the looming global energy crisis.

This study is the first to investigate the application of green synthesized ZnO NPs in *Sorghum bicolor* plant growth under salt stress. To better understand the effects of ZnO NPs as biostimulants, we evaluated their efficiency under normal and high salt (400 mM NaCl) stress conditions by analyzing growth attributes, anatomical structure, and the content of macronutrients. The extent of oxidative stress and the scavenging capacity on sorghum were also evaluated.

2. Materials and Methods

2.1. Preparation of the Plant Extract and the Green Synthesis of Zinc Oxide Nanoparticles

The synthesis of ZnO NPs completed in this study followed the original method described in [29] with modifications. *Agathosma betulina* (Buchu leaves) were purchased online at the Natural Essential Products Ltd. [<https://essentiallynatural.co.za> (accessed on 20 March 2020)] and used to prepare the green extract, which served as the capping agent [30]. About 10 g of grounded Buchu leaves were mixed with 250 mL distilled water (dH₂O) and boiled at 80 °C for 2 h. The mixture was filtered and centrifuged for 10 min at 6000 rpm and the supernatant was collected and used immediately or stored at 4 °C for further use.

Zinc nitrate hexahydrate (N₂O₆Zn) purchased from Sigma-Aldrich (Cat# 96482-500G, Lot # BCBJ7666V) was used as a precursor for the synthesis of ZnO nanoparticles (NPs). Synthesis was initiated by adding 3 g of Zinc nitrate into 250 mL of aqueous Buchu leaf extract and the mixture was boiled at 80 °C for 5 h. A color change of the mixture from pale yellow to dark brown appeared signifying the formation of ZnO NPs [31]. Synthesized ZnO NPs were freeze-dried to obtain ZnO NPs in powdered form, then calcined at 600 °C for 2 h to obtain a more crystallized structure of the nanoparticles. White powdered ZnO NPs were obtained and stored in airtight containers at room temperature when not in use or until further processing.

2.2. Characterization of Zinc Oxide Nanoparticles

The formation of the ZnO NPs was confirmed using Ultraviolet-Visible spectroscopy (Nicolett Evolution 100 from Thermo Electron Corporation, Johannesburg, South Africa) by observing peak formation within the 200–700 nm wavelength range. The phytochemical compositions that participated in the synthesis and the newly formed chemical compositions were determined using Fourier-transform infrared (FTIR) spectroscopy (PerkinElmer Spectrum 100-FTIR Spectrometer from PerkinElmer (Pty) Ltd., Midrand, South Africa) using a 400 to 4000 cm^{-1} spectral range. The morphology and size of the nanoparticles were determined using High-Resolution Scanning Electron Microscopy (Zeiss Auriga HR-SEM purchased from Carl Zeiss Microscopy GmbH, Jena, Germany), the quantity and presence of ZnO NPs were determined on SEM using Energy Dispersive X-ray Spectroscopy (EDX) performed on the Zeiss Auriga detector (Oxford Link-ISIS 300, Concord, MA, USA) [32], and High-Resolution Transmission Electron Microscopy (HRTEM) (Tecnai G2 F20 X-Twin HR-TEM purchased from FEI Company, Hillsboro, OR USA).

The phase purity and particle size of ZnO NPs were determined using the X-ray diffractometer, Bruker AXS (Germany) D8 advanced diffractometer unit. The Scherrer's equation (Equation (1)) was used to determine the crystalline size of the synthesized ZnO NPs [33]:

$$D = \frac{0.9\lambda}{\beta \cos \theta} \quad (1)$$

where D is the crystallite size, λ is the wavelength of x -ray used (1.5406 Å), β is the full width at half maximum (FWHM), and θ is the Bragg's angle.

2.3. Sorghum Seed Germination and Growth Conditions

Sorghum (*Sorghum bicolor* L. Moench) seeds purchased from Agricol, Brackenfell Cape Town, South Africa were disinfected as described previously [24].

For priming treatments, seeds were imbibed in distilled water (ddH₂O) only as the control and 5 and 10 mg/L ZnO NPs solutions for experiments. This was followed by overnight incubation in the dark at 25 °C with shaking at 600 rpm. Seeds were dried under the laminar flow and sown on filter paper placed on a plastic container (28 × 21 and 6 cm height) containing 50 mL of ddH₂O and germinated in the dark at 25 °C for 7 days.

Germinated seeds were sown on pots of sizes (18 × 14 and 6 cm height) and put inside a vessel container sized (21 × 16 and 5 cm height) containing a mixture of potting soil and vermiculite (2:1) and grown in the green house under controlled conditions (26 °C/22 °C day/night; 16 h/8 h light/dark regimes). After 14 days of growth, sorghum plants were treated with 100 mL of salt solution (400 mM NaCl-containing solution) every second day for 7 days. Sorghum plants were harvested on day seven after treatment, rinsed thoroughly with dH₂O and used immediately or stored at −80 °C for future use.

2.4. Growth Parameters

Shoot lengths were measured using a ruler in the mm range. Fresh weights (FW) of the shoots were weighed using a Mettler Toledo AE50 analytical balance (Marshall Scientific, Hampton, VA, USA). Dry Weights (DW) were determined after oven-drying the shoots at 70 °C for 72 h until a constant weight was obtained.

The anatomical structure (epidermis, xylem, and phloem) and element distribution were analyzed at the University of Cape Town, South Africa using High Resolution Scanning Electron Microscopy (HRSEM) and HRSEM-EDX as previously described in [34,35]. All spectra were analyzed using the built in Oxford Inca software suite. Samples were then imaged and collected using a Tescan MIRA field emission gun scanning electron microscope, operated at an accelerating voltage of 5 kV using an in-lens secondary electron detector.

2.5. Physiological and Biochemical Analysis

All spectrophotometric measurements in this study were performed using a Helios[®] Epsilon visible 8 nm bandwidth spectrophotometer (Thermo scientific Waltham, MA, USA) unless otherwise stated.

2.5.1. Histochemical Detection of Reactive Oxygen Species (ROS)

Histochemical detection of ROS was determined as described by [15]. For the detection of superoxide ($O_2^{\bullet-}$), leaves were immersed in 0.1% Nitroblue tetrazolium chloride (NBT) solution and incubated at 25 °C for 2 h in the dark.

The detection of H_2O_2 was performed by immersing sorghum leaves in 1 mg/mL 3',3'-diaminobenzidine (DAB) solution and the mixture was incubated overnight in the dark. After incubation, all histochemical samples were boiled in 80% ethanol at 90 °C for 15 min to remove chlorophyll.

2.5.2. Malondialdehyde Content

Lipid peroxidation was determined by measuring malondialdehyde (MDA) content using the method described in [36]. A total of 100 mg of fresh sorghum plant materials were homogenized in 1 mL of 0.1% trichloroacetic acid (TCA (*w/v*)). Tubes were vortexed to mix well and centrifuged at 13,000 rpm (4 °C) for 10 min. Small holes were created in the cap of the 2 mL Eppendorf tubes using a syringe needle to prevent the tubes from bursting due to pressure from the heat. About 400 μ L of the supernatant was added into a 2 mL Eppendorf tube containing 1 mL of 0.5% TBA, followed by boiling at 80 °C in a water bath for 30 min. After incubation, the tubes were placed on ice for 5 min and centrifuged for another 5 min at 13,500 rpm (4 °C) to precipitate any remaining TBA. About 200 μ L of the supernatant was transferred into a 96 well microtiter plate. The optical density was measured spectrophotometrically at 532 nm and 600 nm.

2.5.3. Fourier-Transform Infrared Spectroscopy (FTIR) Analysis of Biomolecules

The FTIR spectrum of the sorghum shoots was analyzed using a PerkinElmer Spectrum 100-FTIR Spectrometer [PerkinElmer (Pty) Ltd., Midrand, South Africa]. About 2 g of dry sorghum shoot tissues was analyzed where a wider window between 450 and 4000 cm^{-1} was considered.

2.5.4. Enzyme Activity Assays

Enzyme extraction was performed as described by the authors of [37], with a slight modification. About 100 mg of grounded sorghum plant material was homogenized in 100 mM sodium phosphate buffer (pH 8.0). The homogenized samples were centrifuged at 9000 rpm for 20 min at 4 °C. The supernatant was collected and was stored at 4 °C for future use. Activities of selected antioxidant enzymes including Superoxide dismutase (SOD, EC, 1.15.1.11), were estimated as described in [38]. Catalase (CAT, EC 1.11.16) and Ascorbate peroxidase (APX, EC 1.11.1.11) were estimated as described previously [38–40].

2.5.5. Proline Content

Proline content was measured as described in [34,41] with slight modifications. To be specific, pure proline was used as the standard to construct the standard curve instead of using the traditional toluene solution.

2.6. Statistical Analysis

All experiments were repeated at least four times and the data were statistically analyzed by the two-way ANOVA using GraphPad prism 9 (<https://www.graphpad.com> (accessed on 20 October 2021)). Data in the Figures and Tables represent the mean \pm standard deviation. Statistical significance between the control and treated plants was determined by the Bonferroni's multiple comparison test and represented as *** = $p \leq 0.001$, ** = $p \leq 0.01$, and * = $p \leq 0.05$.

3. Results

3.1. Characterization of Zinc Oxide Nanoparticles

The Ultraviolet-Visible absorption spectra were used to determine the optical properties of the green-synthesized ZnO NPs (Figure S1A). Initially, the color of the reaction mixture was pale yellow, which changed to dark brown indicating the formation of nanoparticles. ZnO NPs and Buchu extracts have a wide absorption value and strong absorption peaks at 370 nm and 320 nm, respectively (Figure S1B).

Fourier-transform infrared spectroscopy (FTIR) investigated the functional groups of the phytoconstituents found in the Buchu extract that were responsible for capping and stabilizing the nanoparticles (Figure 1A). The spectrum revealed several bands from 500 to 4000 cm^{-1} . Both the Buchu extract (black line) and the ZnO NPs (red line) spectra exhibited strong peaks including those attributed to the O-H stretch, hydroxyl group, and H-bond (3427 cm^{-1}), to the C-H stretch (2926 cm^{-1}), and the C=C alkene group (1386 cm^{-1}). Some weak peaks were also observed at 1500 cm^{-1} and 1437 cm^{-1} that were attributed to the C=C and aromatic compound and at 1062 cm^{-1} attributed to the OH bending group. The spectrum evidently indicated ZnO NPs formation with an absorption peak at 460 cm^{-1} .

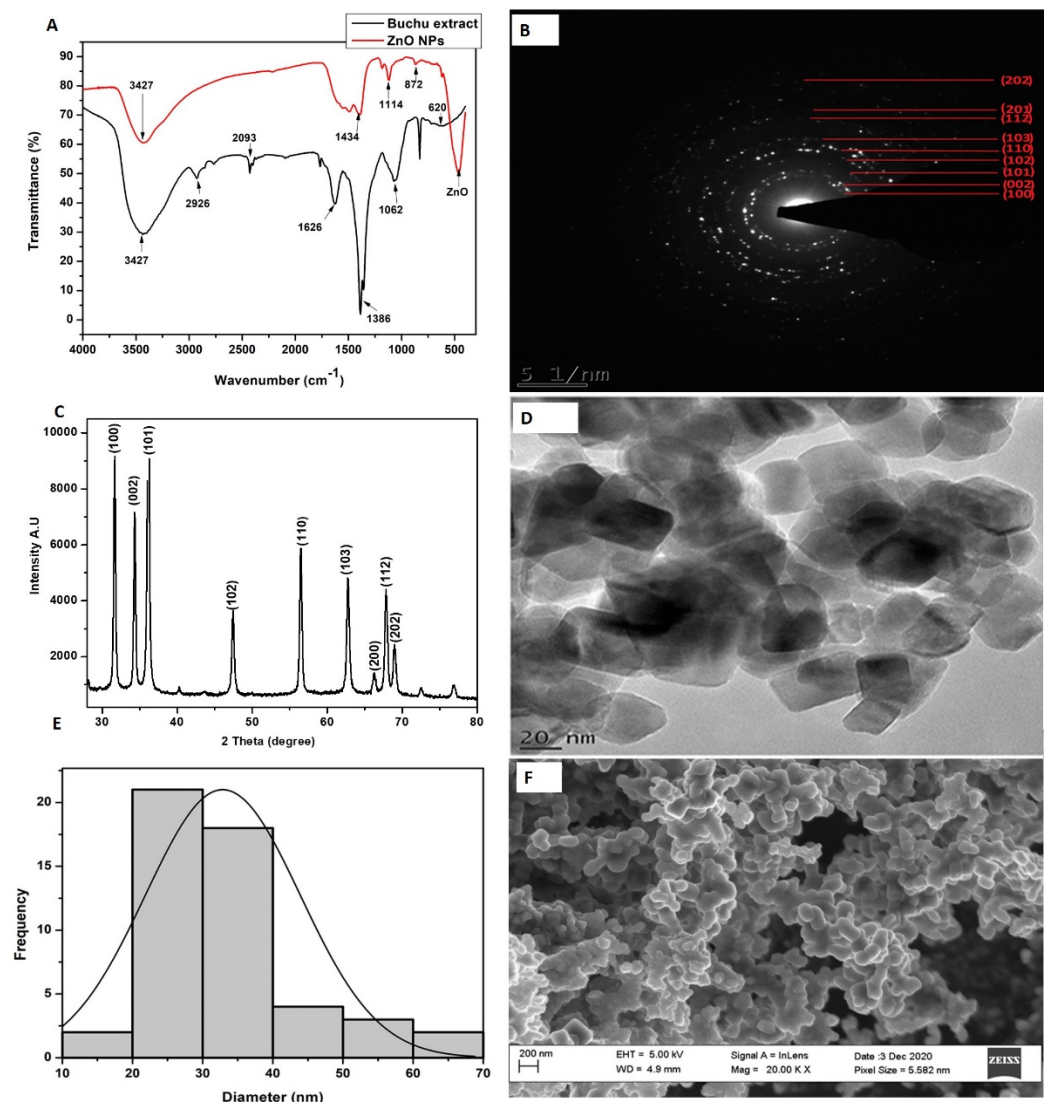


Figure 1. Optical and structural characterization of green-synthesized ZnO NPs using (A) FTIR, (B) SAED, (C) XRD, (D) HRTEM, (E) HRTEM micrograph, and (F) HRSEM analysis.

The selected area diffraction (SAED) pattern (Figure 1B) revealed diffraction peaks at (31.7°) , (34.38°) , (36.21°) , (47.52°) , (56.54°) , (62.84°) , (66.90°) , (67.95°) , and (69.05°) , and were assigned to the (100), (002), (101), (102), (110), (103), (200), (112), and (201) planes on the *x*-ray Diffraction (XRD) spectrum (Figure 1C), respectively. The XDR spectrum of the synthesized ZnO NPs confirmed that the diffraction peaks were well matched with the hexagonal wurtzite structure of ZnO of the Joint Committee on Powder Diffraction Standards (JCPDS) Card Number 36-1451) as shown in Figure 1C and as described previously [42,43].

The average particle size of the prepared ZnO NPs as calculated based on the Debye-Scherrer's formula was 26 nm and matched with the TEM micrograph, which revealed the size of ZnO NPs to be between 20 nm and 30 nm (Figure 1E). HRTEM (Figure 1D) and HRSEM (Figure 1F) images of ZnO NPs revealed that the ZnO NPs were hexagonal, spherical, were of a granular nature and were agglomerated. The EDX spectrum indicated a high percentage of zinc and oxygen, which confirmed the presence of the elemental zinc and the oxygen signal from the ZnO NPs with a weight composition of 82.69% and 17.31%, respectively (Figure S1C).

3.2. The Effect of Salt and the Priming of the ZnO NPs on the Growth Attributes of *S. bicolor*

Plant growth was severely affected by salt stress (Figure 2A), as confirmed by a significant decrease in shoot length (46%) and fresh weight (73.75%) under salt stress (Figure 2B). However, a significant increase in shoot length was observed in plants primed with 5 mg/L (40.9%) and 10 mg/L (51.3%) ZnO NPs when treated with salt (Figure 2B). There was also a significant increase in the fresh weights of salt-treated plants when primed with 5 mg/L (38%) and 10 mg/L (60%) ZnO NPs (Figure 2C). There were no significant changes in the dry weights of all samples.

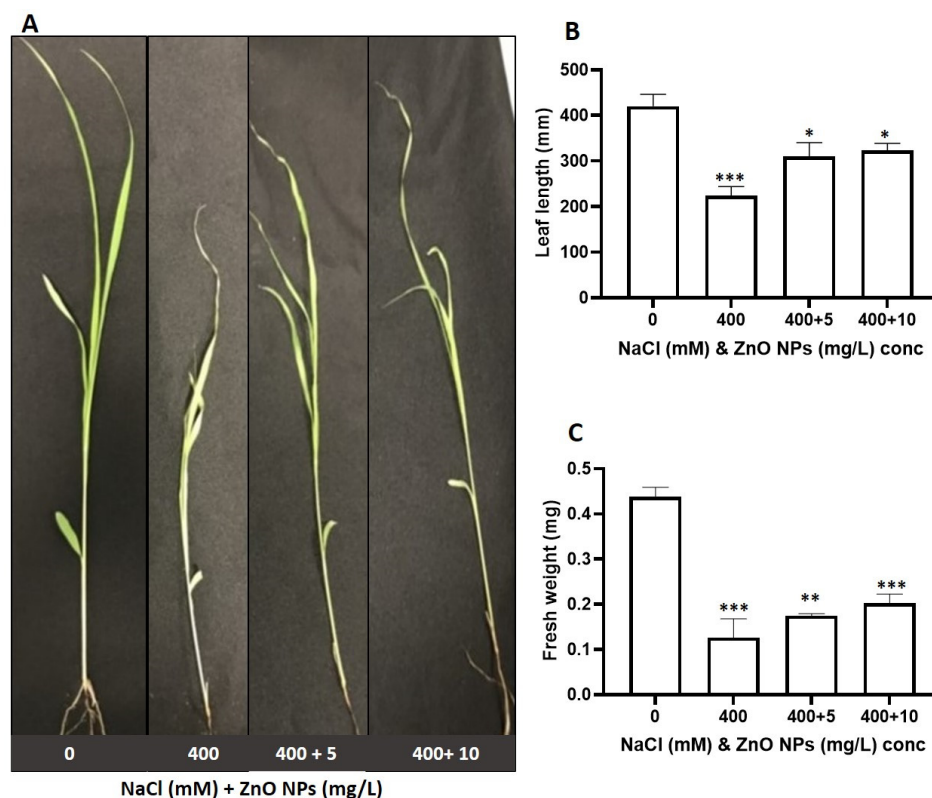


Figure 2. Effect of salt and the priming of the ZnO NPs on the growth parameters of sorghum. (A) Visual image, (B) shoot length, and (C) shoot fresh weight of sorghum plants in response to salt and the priming of the ZnO NPs. Error bars represent the SD calculated from three biological replicates. Statistical significance between the control and treated plants was determined by a two-way ANOVA performed on GraphPad 9.2.0, shown as *** = $p \leq 0.001$ ** = $p \leq 0.01$, and * = $p \leq 0.05$ according to the Bonferroni's multiple comparisons test.

To further understand the effect of salt stress and ZnO NPs on the growth of sorghum, the anatomical structure (epidermis, xylem, and phloem) and element distribution were analyzed using HRSEM and HRSEM/-EDX (Figure 3). HRSEM images revealed well-arranged and smooth epidermis layers in control (0 mM NaCl) plants (Figure 3A), whereas the epidermis from salt-treated plants revealed severe damage and showed signs of shrinkage (Figure 3B). Sorghum shoots from seeds that were primed with ZnO NPs before salt treatment showed an improvement as demonstrated by less deformation and shrinkage of the epidermis especially for the 5 mg/L ZnO NPs treatment (Figure 3C,D). The vascular bundle consisting of the xylem and phloem layers plays a significant role in the transport of water and nutrients [44]. The results revealed large, round, and wider openings of the xylem (Figure 3E, xylem presented by red arrows and phloem presented by white arrows), whereas the xylem of salt-treated sorghum plants was oval shaped, as if the walls had collapsed (Figure 3F). The xylem layers of the sorghum plants primed with ZnO NPs before salt treatment showed an improved surface structure and wider and round openings for both ZnO NPs concentrations (Figure 3G,H).

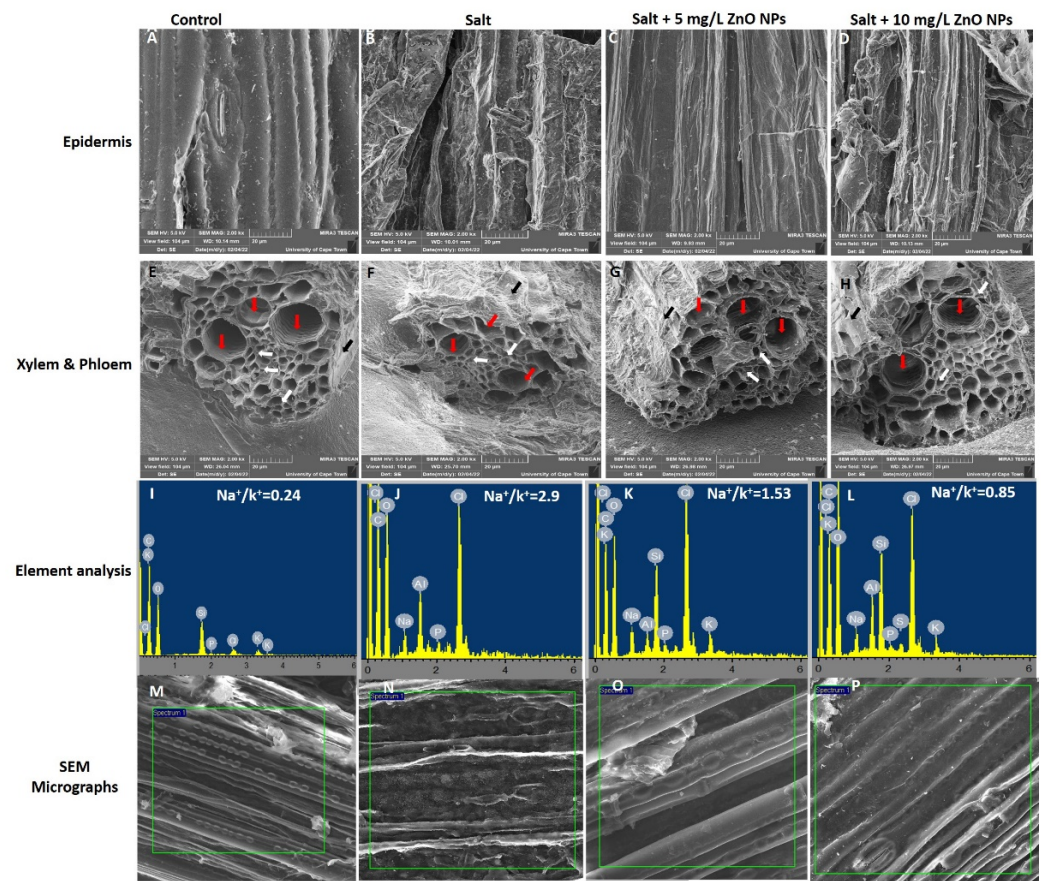


Figure 3. Effect of salt and the priming of the ZnO NPs on the anatomy and element distribution in sorghum plants. (A–D) Epidermis layers, (E–H) Xylem and phloem, (I–L) element content, (M–P) SEM micrographs for the EDX-investigated area.

The effect of salt and ZnO NPs on the absorption and transport of macronutrients was determined by analyzing the element distribution using HRSEM/-EDX, and more importantly, focusing on the Na^+ and K^+ and hence calculating the Na^+/K^+ ratio based on the Weight% (Figure 3I–L; Table S1). Sorghum plants treated with salt resulted in a 1.31-fold increase in Na^+ , whereas the K^+ content decreased by 1.0-fold resulting in a Na^+/K^+ ratio of 2.9 (Figure 3J) as compared to the control ($\text{Na}^+/\text{K}^+ = 2.13$; Figure 3I). Priming with ZnO NPs prior to salt treatment resulted in a 0.56-fold decrease in Na^+ , followed by a low Na^+/K^+ ratio of 1.53 (5 mg/L) (Figure 3K) and 0.85 (10 mg/L) (Figure 3L), when compared

to plants treated with salt only (Figure 3I). SEM images for the EDX investigated area revealed significant morphological changes (Figure 3M–P). HRSEM images for control plants showed a smooth surface area (Figure 3M) as compared to the salt-treated plants (Figure 3N), which showed severe shrinkage. SEM images from the seedlings primed with ZnO NPs prior to salt treatment also revealed smooth epidermis layers with an improved surface area and less deformation (Figure 3O,P).

3.3. The Effect of Salt and the Priming of the ZnO NPs on Oxidative Damage in *S. bicolor*

Oxidative damage was determined by assaying the overproduction of Reactive Oxygen Species (ROS), which eventually led to the damage of lipid membranes, and other biomolecules (Figure 4). Histochemical detection of the superoxide anion ($O_2^{\bullet-}$) was performed using NBT whereby the production of $O_2^{\bullet-}$ was observed based on the appearance of blue spots on sorghum leaves (Figure 4A). Salt-treated plants had a high degree of $O_2^{\bullet-}$ production as seen by dark blue spots on the analyzed leaves as compared to the control, whereas the leaves of plants primed with ZnO NPs (5 mg/L and 10 mg/L) had reduced levels of $O_2^{\bullet-}$ under salt treatment (Figure 4A). Overproduction of H_2O_2 was detected using DAB staining, which was observed by the production of dark brownish spots (Figure 4B). Leaves of salt-treated plants exhibited more pronounced dark brownish color spots as compared to the control. However, priming with ZnO NPs (5 mg/L and 10 mg/L), prevented the over-accumulation of H_2O_2 since the dark brown spots were reduced to a higher degree as compared to the leaves of plants treated with salt only.

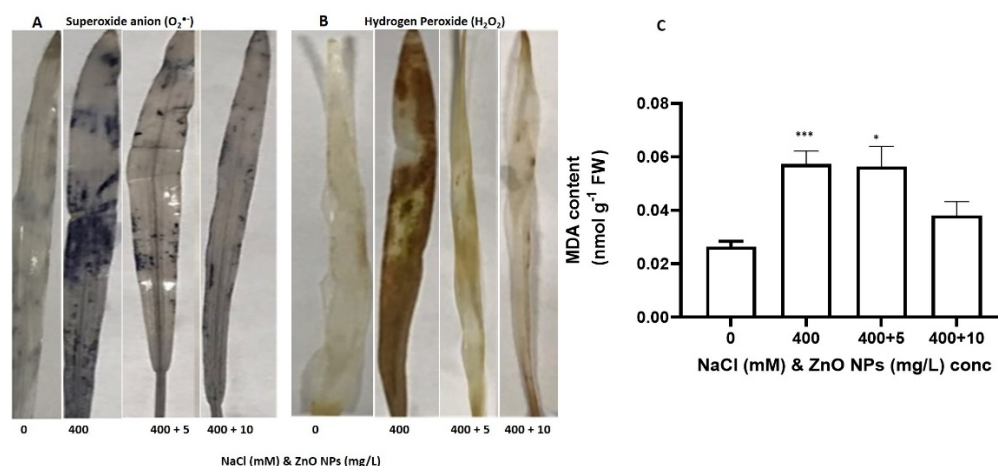


Figure 4. Effect of salt and the priming of ZnO NPs on ROS ($O_2^{\bullet-}$ and H_2O_2) accumulation and MDA content in sorghum. Histochemical detection of (A) $O_2^{\bullet-}$ and (B) H_2O_2 . (C) Measurement of MDA content in salt-treated plants and salt-treated plants primed with ZnO NPs. Error bars represent the SD calculated from three biological replicates. Statistical significance between control and treated plants was determined by a two-way ANOVA performed on GraphPad 9.2.0, shown as *** = $p \leq 0.001$ and * = $p \leq 0.05$ according to the Bonferroni's multiple comparisons test.

Malondialdehyde content was measured to determine the extent of the oxidative damage on membrane lipids (Figure 4C). The results showed that a high salt concentration (400 mM NaCl) significantly increased MDA content by 115.38% as compared to the control. This indicates that salt stress caused significant and serious damage to sorghum membranes. Priming with 5 mg/L showed no difference, but 10 mg/L ZnO NPs decreased the MDA content by 32% in salt-treated plants, indicating the effectiveness of the ZnO NPs to protect plants from severe damage caused by salt.

To understand the effect of salt on the damage to the biomolecules, including carbohydrate, proteins, lipids, and phenolics, this study used FTIR spectroscopy and analyzed a wide spectral region from 450 to 4000 cm^{-1} , which was consistent in all samples (Figure 5). Peaks at 2916.39, 2103.69, and 1637.12 cm^{-1} showed the C-H and $C=C$ - stretching vibration, confirming the presence of alkanes and alkenes, respectively, thus confirming the

presence of carbohydrates. The peak at 1370.74 cm^{-1} can be assigned a C-F stretching vibration for the alkyl halide group. Proteins were confirmed by the presence of amines seen by peaks at 1250.84 cm^{-1} and 1050.68 cm^{-1} (assigned C-N stretching, confirming the presence of aliphatic amines) and 899.62 cm^{-1} and 582.11 cm^{-1} (assigned N-H stretching vibration, confirming the presence of primary and secondary amines). These peaks were consistent in all samples, but big shifts were observed in the peaks that corresponded to carbohydrates and proteins between in all samples. Pronounced differences in the FTIR spectrum of control (black line) plants and those treated with salt only (red line) were clearly observed. Priming with 10 mg/L ZnO NPs (green) showed a better improvement in the spectral peak shift as compared to priming with 5 mg/L ZnO NPs (blue line) in salt-treated sorghum plants.

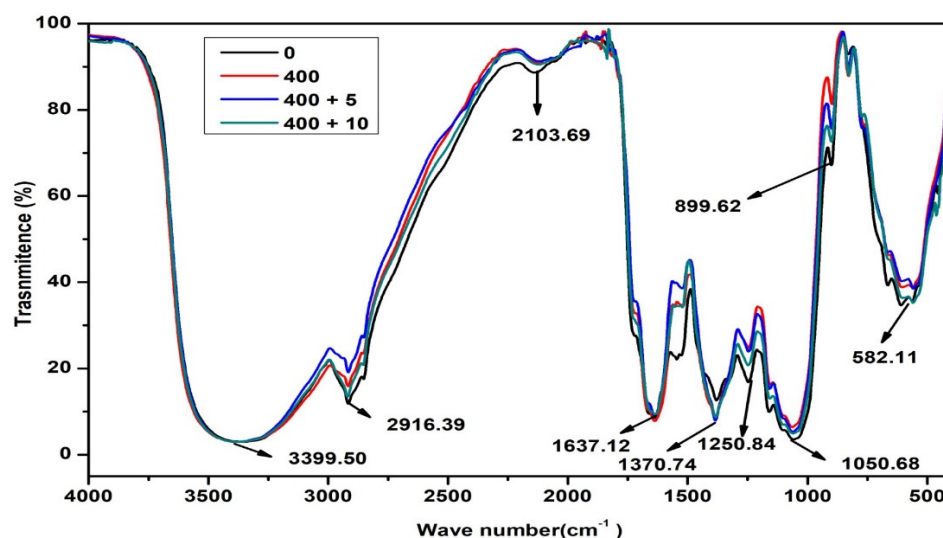


Figure 5. FTIR analysis of the effect of salt and the priming of the ZnO NPs on biomolecules in sorghum plants. Control (0 mM NaCl) plants (black), 400 mM NaCl /salt-treated (red), salt-treated plants primed with 5 mg/L ZnO NPs (blue) and 10 mg/L (green) ZnO NPs.

3.4. Effect of Salt and the Priming of the ZnONPs on the Antioxidative Capacity of *S. bicolor*

Salt markedly increased the antioxidant capacity of sorghum plants by inducing the activities of SOD (170%), CAT (131%), and APX (208%) as compared to their controls (Figure 6A–C). Priming with 5 mg/L ZnO NPs significantly reduced the antioxidant activities of SOD (58%), CAT (90%), and APX (61%), whereas priming with 10 mg/L ZnO NPs reduced the activities of SOD (68%) and APX (66%) (Figure 6B) to a higher degree, except for CAT (Figure 6C).

3.5. Effect of Salt and the Priming of ZnO NPs on the Osmoregulation in *S. bicolor*

Osmolytes such as proline and soluble sugars were analyzed to determine the level of osmotic balance in sorghum plants under salt (400 mM NaCl) stress and the effect of priming with ZnO NPs (Figure 7). Salt stress induced the accumulation of proline by 200% as compared to the control (Figure 7A). Compared with plants treated with salt only, plants primed with ZnO NPs prior to salt treatment resulted in very low proline content of 59.45% for 5 mg/L and 60.29% for 10 mg/L ZnO NPs priming (Figure 7A). Salt stress also induced the accumulation of soluble sugars by 160.60%, as compared to the control (Figure 7B). The priming of ZnO NPs had no significant effect on the content of soluble sugars (Figure 7B).

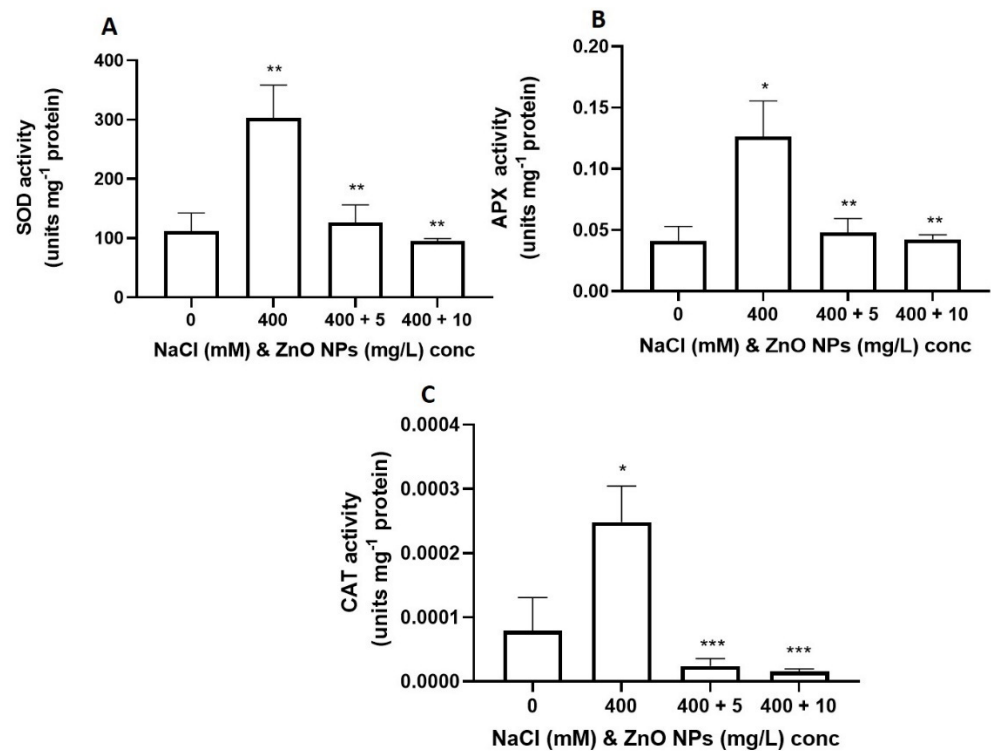


Figure 6. Effect of salt and the priming of ZnO NPs on the antioxidant enzyme activities of sorghum. (A) Superoxide Dismutase, (B) Ascorbate peroxidase and (C) Catalase activity in salt-treated plants, and those primed with ZnO NPs. Error bars represent the SD calculated from three biological replicates. Statistical significance between control and treated plants was determined by a two-way ANOVA performed on GraphPad 9.0, shown as *** = $p \leq 0.001$, ** = $p \leq 0.01$, and * = $p \leq 0.05$ according to the Bonferroni's multiple comparisons test.

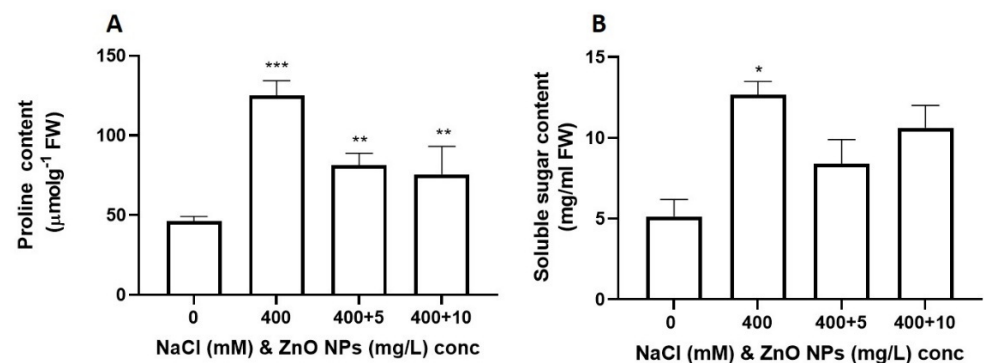


Figure 7. Effect of salt and ZnO NPs on osmolyte accumulation in sorghum. (A) Proline content and (B) soluble sugars in salt-treated plants and those primed with ZnO NPs. Error bars represent the SD calculated from three biological replicates. Statistical significance between control and treated plants was determined by a two-way ANOVA performed on GraphPad 9.2.0, shown as *** = $p \leq 0.001$, ** = $p \leq 0.01$, and * = $p \leq 0.05$ according to the Bonferroni's multiple comparisons test.

4. Discussion

In this study, ZnO NPs were synthesized following a green synthesis method using *Agathosma betulina* (Buchu) extract, which acted as a capping or reducing agent and a precursor for zinc nitrate [30,45–47]. As zinc nitrate was added to the extract, the color changed from pale yellow to dark brown, which indicated the formation of ZnO NPs [48].

The formation of ZnO NPs was further confirmed by observing the absorption peak at ~370 nm (Figure S1A). This is consistent with previous studies, which reported the

absorption of ZnO NPs between 320 nm and 370 nm when synthesized using *Atalantia monophylla* [29], *Cinnamomum Tamala* leaf [49], and *Averrhoa bilimbi* (L) [50].

The FTIR spectra revealed the chemical bands that coded for physiochemical properties found in the plant extract that were responsible for the reduction process to form ZnO NPs as described previously [51]. The disappearance of 2926 and 2093 cm^{-1} spectral bands and the reduction in the intensity of other bands (1060 and 872 cm^{-1}) in ZnO NPs confirmed that phytochemicals were responsible for the reduction of irons to form NPs [31,52]. This was further confirmed by the appearance of the peak at 460 cm^{-1} that can be attributed to the presence of hexagonal wurtzite ZnO NPs, as reported in previous studies, which indicated that ZnO NPs exhibited peaks with similar shapes within the range of 400 to 680 cm^{-1} .

The size and structure of the synthesized ZnO NPs was estimated to be 26.03 nm and the hexagonal, spherical, granular nature, and agglomerated shape is due to the polarity and electrostatic attraction of the ZnO NPs [3]. These nanoparticles were proven to be pure and polycrystalline in nature as analyzed by the SAED and XRD. Similar trends were also observed in other studies where ZnO NPs were synthesized from *Phoenix roebelenii* [5] and *Cissus quadrangularis* [28].

Salinity is one of the major abiotic stresses affecting crop production causing over 50% of agricultural losses [37]. *Sorghum bicolor* is an important staple food crop worldwide widely grown in arid and semi-arid regions [53,54]; thus, it is important to prevent yield losses and maintain its growth and production. The present study demonstrated for the first time the positive effects of priming with green-synthesized ZnO NPs to mitigate the effects of salt stress on the growth of *Sorghum bicolor*, as observed by enhanced growth and an overall tolerance to salt stress. Most studies have demonstrated the exogenous application of nanoparticles (NPs) to mitigate abiotic stress including chilling on *Oryza Sativa* L [29], drought on tomatoes [4,18], salinity on *Glycine max* [7], *Lycopersicon esculentum* [23], *Eleusine coracana* L [55], *Brassica napus* [6] and *Abelmoschus esculentus* L. Moench [8].

Salt stress significantly reduced the growth attributes of sorghum plants including plant height, shoot length, and fresh weight (Figure 2). However, plants primed with ZnO NPs (5 mg/L and 10 mg/L) showed substantial growth improvement compared to non-primed plants under salt stress. The reduced growth might be due to osmotic stress, which affects the absorption and transport of nutrients and water resulting in declined turgidity and cell expansion; hence, reducing growth [56]. The reduced growth might also be due to the diversion of energy meant for growth to homeostasis and other metabolic processes [57], and this is supported by the correlation observed between reduced growth and the high content of osmolytes (Figure 7) in salt-treated sorghum plants.

The anatomical structure of salt-treated sorghum plants was severely affected (Figure 3A,B). The epidermis is an important tissue on the leaf that prevents water loss and invasion by pathogens, while the vascular bundle (xylem and phloem) participates in the transport of water and nutrients [58,59]. Both these structures showed shrinkage and deformation in salt-treated sorghum plants, while these effects were reversed in ZnO NPs-primed plants. Taken together these observations clearly suggest the role of ZnO NPs in promoting plant growth in harsh environments by protecting tissues that are important for transport of nutrients. This is true since Zn is a key element required for plant growth and development by mediating the biosynthesis of growth hormones and eventually activating cell division and enlargement [60,61].

The study further investigated the distribution of macronutrients (Figure 3C,D; Table S1) to understand the growth reduction induced by salt stress and its link with the affected anatomical structure. A correlation between the increase in toxic ions (Na^+ and Cl^-) and a decrease in the absorption of essential elements that are required for growth was observed in this study and this is evident by the high Na^+/K^+ ratio of 2.9 for salt-treated sorghum plants. Surprisingly, element distribution was improved in ZnO NPs-primed sorghum plants under salt stress, and this was supported by a decrease in the Na^+/K^+ ratio of 1.53 (5 mg/L ZnO NPs) and 0.85 (10 mg/L ZnO NPs). SEM micrographs of the

investigated areas corroborated the element distribution, as shown by substantial changes in the morphology of the epidermis associated with shrinkage in salt-treated sorghum plants. This is true since salt stress causes membrane damage due to oxidative stress and these effects were reversed by priming with ZnO NPs. This result is supported by the role of Zn in maintaining membrane integrity, reducing the entry of toxic ions, mediating the translocation of nutrients, and thus maintaining cellular homeostasis [62–66].

To gain more insights into the effect of salt stress and the effectiveness of ZnO NPs on the growth of sorghum, this study also aimed to determine the extent of oxidative damage by assaying ROS accumulation, lipid peroxidation (Figure 4), and damage to biomolecules (Figure 5). When plants are exposed to abiotic stresses, they are generally associated with a high accumulation of free radicals, which induces the activity of antioxidants to regulate homeostasis and reduce lipid peroxidation [20]. ROS (e.g., H_2O_2) are signaling molecules at physiological levels, but their overproduction leads to the oxidative damage of membranes by increasing lipid peroxidation and causes damage to biomolecules [26,49]. Following the morphological attributes, sorghum plants treated with salt accumulated high levels of ROS and MDA, whereas in ZnO NPs-primed sorghum plants, low levels of these markers were observed. Any damage to the biomolecules was assessed using FTIR to inspect any shift in the spectral peaks of sorghum shoots (Figure 5). The FTIR spectra indicated that biomolecules in salt-treated sorghum plants were degraded, since shifts in the spectral peaks corresponding to carbohydrates (2916.39 , 2103.69 , and 1637.12 cm^{-1}) and proteins (1250.84 cm^{-1} , 1050.68 cm^{-1} , 899.62 cm^{-1} , and 582.11 cm^{-1}) were observed [65]. Only the peaks from the 10 mg/L ZnO NPs-primed sorghum plants were closer to those of the control, suggesting that the priming of ZnO NPs reduced salt-induced oxidative stress improving sorghum's response to salt stress and preventing the degradation of biomolecules.

ROS production induces the expression of antioxidant genes, leading to an increase in antioxidants, which enhance the scavenging capacity of ROS at the cellular level; hence, conferring tolerance against stress [67,68]. The results showed that the activities of superoxide dismutase (SOD), catalase (CAT), and ascorbate peroxidase (APX) were greatly increased in the sorghum shoots treated with salt (Figure 6). Similarly, other studies have shown the high activities of antioxidant enzymes in plants under salt stress [67,69]. SOD activity was greater than CAT and APX, suggesting that in addition to its role as the first line of defense in ROS scavenging, by converting superoxide anion ($O_2^{\bullet-}$) into H_2O_2 [6], SOD is a major contributor to the mediation of salt tolerance in sorghum. H_2O_2 is scavenged by peroxidases and catalase; however, APX has a higher affinity for H_2O_2 than CAT [70,71]. In this study, high APX activity was observed than CAT, suggesting that APX played a principal role in scavenging H_2O_2 as observed previously in sorghum [28,34]. In sorghum plants primed with ZnO NPs under salt stress, the activities of antioxidant enzymes significantly decreased, suggesting that ZnO NPs were effective in reducing the production of ROS; thus, preventing oxidative damage [20]. This is consistent with other studies as the application of ZnO NPs induced a tolerance to salt stress in soybeans [7], *Brassica napus* [6], and *Abelmoschus esculentus* L. Moench [8].

Plants also survive stress through osmoregulation controlled by the accumulation of osmolytes including proline, soluble sugars, and glycine, to promote an osmotic balance at cellular level [72,73]. A significant increase in proline and soluble sugars was observed in salt-treated sorghum plants as compared to control plants; however, ZnO NPs-primed sorghum plants showed a reduced proline content with no significant changes observed for soluble sugars (Figure 7). Proline is an important signaling molecule that functions as a molecular chaperone by stabilizing and protecting membranes and proteins under abiotic stresses [70]. While soluble sugars play a similar role to proline as osmoprotectants [20], their level remained the same in ZnO NPs-primed sorghum plants under salt stress (Figure 7D). These results indicated that priming with ZnO NPs was efficient in improving osmoregulation in sorghum under salt stress, and hence there was no need for the plant to produce a high concentration of osmolytes when primed with ZnO NPs. High

levels of proline under salt stress have been reported previously for sorghum [34,74–76]; however, the role of ZnO NPs in reducing proline content and hence the effects of salt stress in sorghum is reported for the first time in this study. In soybean, priming with ZnO NPs was reported to be efficient in decreasing the proline content under salt stress [7].

A positive correlation was observed between the induction of proline content and the over-accumulation of ROS and the induction of antioxidant enzymes activities under salt stress. Similarly, their reduction in ZnO NPs-primed sorghum plants, might suggest that the accumulation of proline under salt stress was partly stimulated by the accumulation of toxic ions (Na^+ and Cl^-) and ROS. Thus, proline played a dual role to scavenge ROS and promote the activities of the antioxidant enzymes [71,72]. This is true since the ZnO NPs-primed sorghum plants presented exceptionally low levels of these traits to almost the same magnitude as that of the control, suggesting that there was no need for high proline production.

5. Conclusions

In summary, the results of this study indicate that sorghum growth is affected by high salt but priming with ZnO NPs stimulated a tolerance to salt and hence improved growth. Under salt stress, Na^+ over-accumulates in cells and causes osmotic and ionic stress, causing damage to membrane layers and affects the absorption of essential elements such as K^+ into cells. As K^+ is a component of most enzymes, its unavailability disrupts the normal functioning and regulation of cells [77–79]. Thus, these results partly propose that the mechanism of ZnO NPs-induced tolerance in sorghum is that ZnO NPs prevents damage to the epidermal layers and vascular bundle tissue, which leads to minimized water loss, and improved nutrient and water transport. This maintains ion homeostasis, thereby restricting the transport of Na^+ to the shoots and ensuring a low Na^+/K^+ ratio in sorghum shoots. This leads to the proper functioning of cells, prevents ROS accumulation and damage to biomolecules and hence improves sorghum growth under salt stress. However, these observations will require further experimental analysis by assaying the transcripts of genes encoding the Na^+ and K^+ pumps. Most importantly, these results provide a novel insight into the mechanism of the salinity response of sorghum as mediated by priming with ZnO NPs and the use of 10 mg/L is recommended.

Supplementary Materials: The following supporting information can be downloaded at: <https://www.mdpi.com/article/10.3390/agriculture12050597/s1>, Figure S1: Characterization of green-synthesized ZnO NPs using, Ultraviolet-Visible absorption spectra for ZnO NPs and Buchu extract at (A) 400–4000 nm wavelength, (B) 300–500 nm wavelength range, (C) histogram analysis of the size of ZnO NPs, (C), element composition of the ZnO NPs sample; Table S1: Overall element distribution analyzed by SEM-EDX spectroscopy in sorghum shoots.

Author Contributions: Conceptualization, T.M. and R.F.A.; methodology, T.R., N.N., N.M.; software, E.I., T.M. and R.F.A.; validation, T.M., E.I., R.F.A., formal analysis and investigation, T.R., N.N., N.M.; resources, T.M., R.F.A., E.I., data curation, T.M.; writing—original draft preparation, T.R.; writing—review and editing, T.M., N.N., N.M., E.I. and R.F.A., visualization, and supervision, T.M., E.I. and R.F.A.; project administration, T.M., R.F.A., E.I.; funding acquisition, T.M., E.I., R.F.A. All authors have read and agreed to the published version of the manuscript.

Funding: This research was funded by the National Research Foundation of South Africa under the Black Academics Advancement (UID: 112201) and Thuthuka Institutional Funding (UID: 121939, 116258 and 118469), Grants.

Institutional Review Board Statement: Not applicable.

Informed Consent Statement: Not applicable.

Data Availability Statement: Not applicable.

Acknowledgments: We would like to acknowledge the colleagues at the department of Biotechnology, UWC and the SensorLab at Chemical Sciences department, University of the Western Cape, for providing the space and most of the equipment that are situated in the laboratories available for use.

Conflicts of Interest: The authors declare no conflict of interest. The funders had no role in the design of the study; in the collection, analyses, or interpretation of data; in the writing of the manuscript, or in the decision to publish the results.

References

- Chhipa, H. Applications of nanotechnology in agriculture. In *Methods in Microbiology*; Elsevier: Amsterdam, The Netherlands, 2019; pp. 115–142.
- Kumar, V.; Guleria, P.; Kumar, V.; Yadav, S.K. Gold nanoparticle exposure induces growth and yield enhancement in *Arabidopsis thaliana*. *Sci. Total Environ.* **2013**, *461*, 462–468. [[CrossRef](#)] [[PubMed](#)]
- Song, Y.; Jiang, M.; Zhang, H.; Li, R. Zinc Oxide Nanoparticles Alleviate Chilling Stress in Rice (*Oryza sativa* L.) by Regulating Antioxidative System and Chilling Response Transcription Factors. *Molecules* **2021**, *26*, 2196. [[CrossRef](#)] [[PubMed](#)]
- El-Zohri, M.; Al-Wadaani, N.A.; Bafeel, S.O. Foliar Sprayed Green Zinc Oxide Nanoparticles Mitigate Drought-Induced Oxidative Stress in Tomato. *Plants* **2021**, *10*, 2400. [[CrossRef](#)] [[PubMed](#)]
- HariPriya, P.; Stella, P.M.; Anusuya, S. Foliar spray of zinc oxide nanoparticles improves salt tolerance in finger millet crops under glass-house condition. *SCIOL Biotechnol.* **2018**, *1*, 20–29.
- El-Badri, A.M.; Batool, M.; Wang, C.; Hashem, A.M.; Tabl, K.M.; Nishawy, E.; Kuai, J.; Zhou, G.; Wang, B. Selenium and zinc oxide nanoparticles modulate the molecular and morpho-physiological processes during seed germination of *Brassica napus* under salt stress. *Ecotoxicol. Environ. Saf.* **2021**, *225*, 112695. [[CrossRef](#)]
- Gaafar, Y.Z.A.; Ziebell, H. Comparative study on three viral enrichment approaches based on RNA extraction for plant virus/viroid detection using high-throughput sequencing. *PLoS ONE* **2020**, *15*, e0237951. [[CrossRef](#)]
- Alabdallah, N.M.; Alzahrani, H.S. The potential mitigation effect of ZnO nanoparticles on [*Abelmoschus esculentus* L. Moench] metabolism under salt stress conditions. *Saudi J. Biol. Sci.* **2020**, *27*, 3132–3137. [[CrossRef](#)]
- Tsegaye, M.M.; Chouhan, G.; Fentie, M.; Tyagi, P.; Nand, P. Therapeutic Potential of Green Synthesized Metallic Nanoparticles against *Staphylococcus aureus*. *Curr. Drug Res. Rev.* **2021**, *13*, 172–183. [[CrossRef](#)]
- Jamkhande, P.G.; Ghule, N.W.; Bamer, A.H.; Kalaskar, M.G. Metal nanoparticles synthesis: An overview on methods of preparation, advantages and disadvantages, and applications. *J. Drug Deliv. Sci. Technol.* **2019**, *53*, 101174. [[CrossRef](#)]
- Bandeira, M.; Giovanela, M.; Roesch-Ely, M.; Devine, D.M.; Da Silva Crespo, J. Green synthesis of zinc oxide nanoparticles: A review of the synthesis methodology and mechanism of formation. *Sustain. Chem. Pharm.* **2020**, *15*, 100223. [[CrossRef](#)]
- Islam, F.; Shohag, S.; Uddin, M.J.; Islam, M.R.; Nafady, M.H.; Akter, A. Exploring the Journey of Zinc Oxide Nanoparticles (ZnO-NPs) toward Biomedical Applications. *Materials* **2022**, *15*, 2160. [[CrossRef](#)] [[PubMed](#)]
- Agarwal, H.; Kumar, S.V.; Rajeshkumar, S. A review on green synthesis of zinc oxide nanoparticles—An eco-friendly approach. *Resour.-Effic. Technol.* **2017**, *3*, 406–413. [[CrossRef](#)]
- Mirzaei, H.; Darroudi, M. Zinc oxide nanoparticles: Biological synthesis and biomedical applications. *Ceram. Int.* **2017**, *43*, 907–914. [[CrossRef](#)]
- Jiang, J.; Pi, J.; Cai, J. The Advancing of Zinc Oxide Nanoparticles for Biomedical Applications. *Bioinorg. Chem. Appl.* **2018**, *2018*, 1062562. [[CrossRef](#)] [[PubMed](#)]
- Faizan, M.; Bhat, J.A.; Chen, C.; Alyemeni, M.N.; Wijaya, L.; Ahmad, P.; Yu, F. Zinc oxide nanoparticles (ZnO-NPs) induce salt tolerance by improving the antioxidant system and photosynthetic machinery in tomato. *Plant Physiol. Biochem.* **2021**, *161*, 122–130. [[CrossRef](#)] [[PubMed](#)]
- Zulfiqar, F.; Ashraf, M. Nanoparticles potentially mediate salt stress tolerance in plants. *Plant Physiol. Biochem.* **2021**, *160*, 257–268. [[CrossRef](#)]
- Singh, A.; Singh, N.B.; Hussain, I.; Singh, H.; Singh, S.C. Plant-nanoparticle interaction: An approach to improve agricultural practices and plant productivity. *Int. J. Pharm. Sci. Invent.* **2015**, *4*, 25–40.
- Raskar, S.V.; Laware, S.L. Effect of zinc oxide nanoparticles on cytology and seed germination in onion. *Int. J. Curr. Microbiol. Appl. Sci.* **2014**, *3*, 467–473.
- Gupta, S.; Schillaci, M.; Walker, R.; Smith, P.; Watt, M.; Roessner, U. Alleviation of salinity stress in plants by endophytic plant-fungal symbiosis: Current knowledge, perspectives and future directions. *Plant Soil* **2020**, *461*, 219–244. [[CrossRef](#)]
- Thakur, M.; Bhattacharya, S.; Khosla, P.K.; Puri, S. Improving production of plant secondary metabolites through biotic and abiotic elicitation. *J. Appl. Res. Med. Aromat. Plants* **2018**, *12*, 1–12. [[CrossRef](#)]
- Arif, Y.; Singh, P.; Siddiqui, H.; Bajguz, A.; Hayat, S. Salinity induced physiological and biochemical changes in plants: An omic approach towards salt stress tolerance. *Plant Physiol. Biochem.* **2020**, *156*, 64–77. [[CrossRef](#)] [[PubMed](#)]
- Yang, Q.; Chen, Z.-Z.; Zhou, X.-F.; Yin, H.-B.; Li, X.; Xin, X.-F.; Hong, X.-H.; Zhu, J.-K.; Gong, Z. Overexpression of SOS (Salt Overly Sensitive) Genes Increases Salt Tolerance in Transgenic *Arabidopsis*. *Mol. Plant* **2009**, *2*, 22–31. [[CrossRef](#)] [[PubMed](#)]
- Satish, L.; Shilpha, J.; Pandian, S.K.; Rency, A.S.; Rathinapriya, P.; Ceasar, S.A.; Largia, M.J.V.; Kumar, A.A.; Ramesh, M. Analysis of genetic variation in sorghum (*Sorghum bicolor* (L.) Moench) genotypes with various agronomical traits using SPAR methods. *Gene* **2015**, *576*, 581–585. [[CrossRef](#)] [[PubMed](#)]
- Rahman, A.; Nahar, K.; Hasanuzzaman, M.; Fujita, M. Calcium Supplementation Improves Na⁺/K⁺ Ratio, Antioxidant Defense and Glyoxalase Systems in Salt-Stressed Rice Seedlings. *Front. Plant Sci.* **2016**, *7*, 609. [[CrossRef](#)]

26. Foyer, C.H.; Noctor, G. Redox homeostasis and antioxidant signaling: A metabolic interface between stress perception and physiological responses. *Plant Cell* **2005**, *17*, 1866–1875. [[CrossRef](#)]
27. Krishnamurthy, V.; Shukla, J. Intraseasonal and Seasonally Persisting Patterns of Indian Monsoon Rainfall. *J. Clim.* **2007**, *20*, 3–20. [[CrossRef](#)]
28. Costa, P.H.A.D.; Neto, A.D.D.A.; Bezerra, M.A.; Prisco, J.T.; Gomes-Filho, E. Antioxidant-enzymatic system of two sorghum genotypes differing in salt tolerance. *Braz. J. Plant Physiol.* **2005**, *17*, 353–362. [[CrossRef](#)]
29. Thema, F.; Manikandan, E.; Dhlamini, M.; Maaza, M. Green synthesis of ZnO nanoparticles via *Agathosma betulina* natural extract. *Mater. Lett.* **2015**, *161*, 124–127. [[CrossRef](#)]
30. Khan, Z.U.H.; Sadiq, H.M.; Shah, N.S.; Khan, A.U.; Muhammad, N.; Hassan, S.U.; Tahir, K.; Safi, S.Z.; Khan, F.U.; Imran, M.; et al. Greener synthesis of zinc oxide nanoparticles using *Trianthema portulacastrum* extract and evaluation of its photocatalytic and biological applications. *J. Photochem. Photobiol. B Biol.* **2019**, *192*, 147–157. [[CrossRef](#)]
31. Chau, T.P.; Brindhadevi, K.; Krishnan, R.; Alyousef, M.A.; Almoallim, H.S.; Whangchai, N.; Pikulkaew, S. A novel synthesis, analysis and evaluation of *Musa coccinea* based zero valent iron nanoparticles for antimicrobial and antioxidant. *Environ. Res.* **2022**, *206*, 112770. [[CrossRef](#)]
32. Saad, R.; Gamal, A.; Zayed, M.; Ahmed, A.M.; Shaban, M.; BinSabt, M.; Rabia, M.; Hamdy, H. Fabrication of ZnO/CNTs for Application in CO₂ Sensor at Room Temperature. *Nanomaterials* **2021**, *11*, 3087. [[CrossRef](#)] [[PubMed](#)]
33. Holzwarth, U.; Gibson, N. The Scherrer equation versus the 'Debye-Scherrer equation'. *Nat. Nanotechnol.* **2011**, *6*, 534. [[CrossRef](#)] [[PubMed](#)]
34. Mulaudzi, T.; Hendricks, K.; Mabiya, T.; Muthevhuili, M.; Ajayi, R.F.; Mayedwa, N.; Gehring, C.; Iwuoha, E. Calcium Improves Germination and Growth of *Sorghum bicolor* Seedlings under Salt Stress. *Plants* **2020**, *9*, 730. [[CrossRef](#)] [[PubMed](#)]
35. Rui, M.; Ma, C.; Hao, Y.; Guo, J.; Rui, Y.; Tang, X.; Zhao, Q.; Fan, X.; Zhang, Z.; Hou, T.; et al. Iron Oxide Nanoparticles as a Potential Iron Fertilizer for Peanut (*Arachis hypogaea*). *Front. Plant Sci.* **2016**, *7*, 815. [[CrossRef](#)]
36. Nakano, Y.; Asada, K. Hydrogen Peroxide is Scavenged by Ascorbate-specific Peroxidase in Spinach Chloroplasts. *Plant Cell Physiol.* **1981**, *22*, 867–880.
37. Vijayakumar, S.; Mahadevan, S.; Arulmozhi, P.; Sriram, S.; Praseetha, P.K. Green synthesis of zinc oxide nanoparticles using *Atalantia monophylla* leaf extracts: Characterization and antimicrobial analysis. *Mater. Sci. Semicond. Process.* **2018**, *82*, 39–45. [[CrossRef](#)]
38. Ramanarayanan, R.; Bhabhina, N.M.; Dharsana, M.V.; Nivedita, C.V.; Sindhu, S. Green synthesis of zinc oxide nanoparticles using extract of *Averrhoa bilimbi* (L) and their photoelectrode applications. *Mater. Today Proc.* **2018**, *5*, 16472–16477. [[CrossRef](#)]
39. Agarwal, H.; Nakara, A.; Menon, S.; Shanmugam, V. Eco-friendly synthesis of zinc oxide nanoparticles using *Cinnamomum Tamala* leaf extract and its promising effect towards the antibacterial activity. *J. Drug Deliv. Sci. Technol.* **2019**, *53*, 101212. [[CrossRef](#)]
40. Aebi, H. [13] Catalase in vitro. In *Methods in Enzymology*; Elsevier: Amsterdam, The Netherlands, 1984; pp. 121–126.
41. Dhindsa, R.S.; Plumb-Dhindsa, P.; Thorpe, T.A. Leaf Senescence: Correlated with Increased Levels of Membrane Permeability and Lipid Peroxidation, and Decreased Levels of Superoxide Dismutase and Catalase. *J. Exp. Bot.* **1981**, *32*, 93–101. [[CrossRef](#)]
42. Shashanka, R.; Esgin, H.; Yilmaz, V.M.; Caglar, Y. Fabrication and characterization of green synthesized ZnO nanoparticle based dye-sensitized solar cells. *J. Sci. Adv. Mater. Devices* **2020**, *5*, 185–191. [[CrossRef](#)]
43. Al-Kordy, H.M.H.; Sabry, S.A.; Mabrouk, M.E.M. Statistical optimization of experimental parameters for extracellular synthesis of zinc oxide nanoparticles by a novel haloaliphilic *Alkalibacillus* sp. W7. *Sci. Rep.* **2021**, *11*, 1–14. [[CrossRef](#)] [[PubMed](#)]
44. Słupianek, A.; Dolzblasz, A.; Sokolowska, K. Xylem Parenchyma—Role and Relevance in Wood Functioning in Trees. *Plants* **2021**, *10*, 1247. [[CrossRef](#)] [[PubMed](#)]
45. Gupta, M.; Tomar, R.S.; Kaushik, S.; Mishra, R.K.; Sharma, D. Effective Antimicrobial Activity of Green ZnO Nano Particles of *Catharanthus roseus*. *Front. Microbiol.* **2018**, *9*, 2030. [[CrossRef](#)] [[PubMed](#)]
46. Sharmila, G.; Thirumarimurugan, M.; Muthukumar, C. Green synthesis of ZnO nanoparticles using *Tecoma castanifolia* leaf extract: Characterization and evaluation of its antioxidant, bactericidal and anticancer activities. *Microchem. J.* **2018**, *145*, 578–587. [[CrossRef](#)]
47. Ogunyemi, S.O.; Abdallah, Y.; Zhang, M.; Fouad, H.; Hong, X.; Ibrahim, E.; Masum, M.I.; Hossain, A.; Mo, J.; Li, B. Green synthesis of zinc oxide nanoparticles using different plant extracts and their antibacterial activity against *Xanthomonas oryzae* pv. *oryzae*. *Artif. Cells Nanomed. Biotechnol.* **2019**, *47*, 341–352. [[CrossRef](#)]
48. Lyimo, G.V. Green Synthesised Zinc Oxide Nanoparticles and Their Antifungal Effect on *Candida albicans* Biofilms. Master's Thesis, University of the Western Cape, Western Cape, South Africa, 2020.
49. Khan, M.T.; Ahmed, S.; Shah, A.A.; Shah, A.N.; Tanveer, M.; El-Sheikh, M.A.; Siddiqui, M.H. Influence of Zinc Oxide Nanoparticles to Regulate the Antioxidants Enzymes, Some Osmolytes and Agronomic Attributes in *Coriandrum sativum* L. Grown under Water Stress. *Agronomy* **2021**, *11*, 2004. [[CrossRef](#)]
50. Aldeen, T.S.; Mohamed HE, A.; Maaza, M. ZnO nanoparticles prepared via a green synthesis approach: Physical properties, photocatalytic and antibacterial activity. *J. Phys. Chem. Solids* **2022**, *160*, 110313. [[CrossRef](#)]
51. Sathappan, S.; Kirubakaran, N.; Gunasekaran, D.; Gupta, P.K.; Verma, R.S.; Sundaram, J. Green Synthesis of Zinc Oxide Nanoparticles (ZnO NPs) Using *Cissus quadrangularis*: Characterization, Antimicrobial and Anticancer Studies. *Proc. Natl. Acad. Sci. India Sect. B Boil. Sci.* **2021**, *91*, 289–296. [[CrossRef](#)]

52. Afzal, S.; Sharma, D.; Singh, N.K. Eco-friendly synthesis of phytochemical-capped iron oxide nanoparticles as nano-priming agent for boosting seed germination in rice (*Oryza sativa* L.). *Environ. Sci. Pollut. Res.* **2021**, *28*, 40275–40287. [[CrossRef](#)]
53. Rosenow, D.; Quisenberry, J.; Wendt, C.; Clark, L. Drought tolerant sorghum and cotton germplasm. *Agric. Water Manag.* **1983**, *7*, 207–222. [[CrossRef](#)]
54. Punia, S. Barley starch modifications: Physical, chemical and enzymatic—A review. *Int. J. Biol. Macromol.* **2020**, *144*, 578–585. [[CrossRef](#)] [[PubMed](#)]
55. Parihar, P.; Singh, S.; Singh, R.; Singh, V.P.; Prasad, S.M. Effect of salinity stress on plants and its tolerance strategies: A review. *Environ. Sci. Pollut. Res.* **2014**, *22*, 4056–4075. [[CrossRef](#)] [[PubMed](#)]
56. Yadav, A.N. Plant microbiomes for sustainable agriculture: Current research and future challenges. *Plant Microbiomes Sustain. Agric.* **2020**, *25*, 475–482. [[CrossRef](#)]
57. Atkin, O.K.; Macherel, D. The crucial role of plant mitochondria in orchestrating drought tolerance. *Ann. Bot.* **2008**, *103*, 581–597. [[CrossRef](#)]
58. Pacheco-Silva, N.V.; Donato, A.M. Morpho-anatomy of the leaf of *Myrciaria glomerata*. *Rev. Bras. Farm.* **2016**, *26*, 275–280. [[CrossRef](#)]
59. Hwang, B.G.; Ryu, J.; Lee, S.J. Vulnerability of Protoxylem and Metaxylem Vessels to Embolisms and Radial Refilling in a Vascular Bundle of Maize Leaves. *Front. Plant Sci.* **2016**, *7*, 941. [[CrossRef](#)]
60. Ashraf, U.; Mahmood, M.H.-U.; Hussain, S.; Abbas, F.; Anjum, S.A.; Tang, X. Lead (Pb) distribution and accumulation in different plant parts and its associations with grain Pb contents in fragrant rice. *Chemosphere* **2020**, *248*, 126003. [[CrossRef](#)]
61. Elsheery, N.I.; Helaly, M.N.; El-Hoseiny, H.M.; Alam-Eldein, S.M. Zinc Oxide and Silicone Nanoparticles to Improve the Resistance Mechanism and Annual Productivity of Salt-Stressed Mango Trees. *Agronomy* **2020**, *10*, 558. [[CrossRef](#)]
62. Jiang, G.; Keller, J.; Bond, P.L. Bond, Determining the long-term effects of H₂S concentration, relative humidity and air temperature on concrete sewer corrosion. *Water Res.* **2014**, *65*, 157–169. [[CrossRef](#)]
63. Weisany, W.; Sohrabi, Y.; Heidari, G.; Siosemardeh, A.; Ghassemi-Golezani, K. Changes in antioxidant enzymes activity and plant performance by salinity stress and zinc application in soybean (*Glycine max* L.). *Plant Omics* **2012**, *5*, 60–67.
64. He, G.; Wu, Y.; Zhang, Y.; Zhu, Y.; Liu, Y.; Li, N.; Li, M.; Zheng, G.; He, B.; Yin, Q.; et al. Addition of Zn to the ternary Mg–Ca–Sr alloys significantly improves their antibacterial properties. *J. Mater. Chem. B* **2015**, *3*, 6676–6689. [[CrossRef](#)] [[PubMed](#)]
65. Aktaş, H.; Abak, K.; Öztürk, L.; Çakmak, İ. The effect of zinc on growth and shoot concentrations of sodium and potassium in pepper plants under salinity stress. *Turk. J. Agric. For.* **2007**, *30*, 407–412.
66. Tolay, I. The impact of different Zinc (Zn) levels on growth and nutrient uptake of Basil (*Ocimum basilicum* L.) grown under salinity stress. *PLoS ONE* **2021**, *16*, e0246493. [[CrossRef](#)] [[PubMed](#)]
67. Gill, S.S.; Tuteja, N. Reactive oxygen species and antioxidant machinery in abiotic stress tolerance in crop plants. *Plant Physiol. Biochem.* **2010**, *48*, 909–930. [[CrossRef](#)]
68. Venkatachalam, P.; Priyanka, N.; Manikandan, K.; Ganeshbabu, I.; Indiraarulsevi, P.; Geetha, N.; Muralikrishna, K.; Bhattacharya, R.; Tiwari, M.; Sharma, N.; et al. Enhanced plant growth promoting role of phycomolecules coated zinc oxide nanoparticles with P supplementation in cotton (*Gossypium hirsutum* L.). *Plant Physiol. Biochem.* **2017**, *110*, 118–127. [[CrossRef](#)] [[PubMed](#)]
69. Ali, S.; Rizwan, M.; Qayyum, M.F.; Ok, Y.S.; Ibrahim, M.; Riaz, M.; Arif, M.S.; Hafeez, F.; Al-Wabel, M.I.; Shahzad, A.N. Biochar soil amendment on alleviation of drought and salt stress in plants: A critical review. *Environ. Sci. Pollut. Res.* **2017**, *24*, 12700–12712. [[CrossRef](#)]
70. Hayat, S.; Hayat, Q.; Alyemeni, M.N.; Wani, A.S.; Pichtel, J.; Ahmad, A. Role of proline under changing environments: A review. *Plant Signal. Behav.* **2012**, *7*, 1456–1466. [[CrossRef](#)]
71. Mittler, R. Oxidative stress, antioxidants and stress tolerance. *Trends Plant Sci.* **2002**, *7*, 405–410. [[CrossRef](#)]
72. Slama, I.; Abdelly, C.; Bouchereau, A.; Flowers, T.; Savouré, A. Diversity, distribution and roles of osmoprotective compounds accumulated in halophytes under abiotic stress. *Ann. Bot.* **2015**, *115*, 433–444. [[CrossRef](#)]
73. Upadhyaya, H.; Dutta, B.K.; Panda, S.K. Zinc Modulates Drought-Induced Biochemical Damages in Tea [*Camellia sinensis* (L) O Kuntze]. *J. Agric. Food Chem.* **2013**, *61*, 6660–6670. [[CrossRef](#)]
74. El Omari, R.; Ben Mrid, R.; Chibi, F.; Nhiri, M. Involvement of phosphoenolpyruvate carboxylase and antioxidant enzymes in nitrogen nutrition tolerance in *Sorghum bicolor* plants. *Russ. J. Plant Physiol.* **2016**, *63*, 719–726. [[CrossRef](#)]
75. El-Haddad ES, H.; O’Leary, J.W. Effect of salinity and K/Na ratio of irrigation water on growth and solute content of *Atriplex amnicola* and *Sorghum bicolor*. *Irrig. Sci.* **1994**, *14*, 127–133. [[CrossRef](#)]
76. Heidari, A.; Younesi, H.; Mehraban, Z. Removal of Ni(II), Cd(II), and Pb(II) from a ternary aqueous solution by amino functionalized mesoporous and nano mesoporous silica. *Chem. Eng. J.* **2009**, *153*, 70–79. [[CrossRef](#)]
77. Horie, T.; Schroeder, J.I. Sodium Transporters in Plants. Diverse Genes and Physiological Functions. *Plant Physiol.* **2004**, *136*, 2457–2462. [[CrossRef](#)]
78. Ward, P.S.; Patel, J.; Wise, D.R.; Abdel-Wahab, O.; Bennett, B.D.; Collier, H.A.; Cross, J.R.; Fantin, V.R.; Hedvat, C.V.; Perl, A.E.; et al. The Common Feature of Leukemia-Associated IDH1 and IDH2 Mutations Is a Neomorphic Enzyme Activity Converting α -Ketoglutarate to 2-Hydroxyglutarate. *Cancer Cell* **2010**, *17*, 225–234. [[CrossRef](#)]
79. Zhu, J.-K. Salt and drought stress signal transduction in plants. *Annu. Rev. Plant Biol.* **2002**, *53*, 247–273. [[CrossRef](#)]